Finite-temperature phase diagram of a spin-polarized ultracold Fermi gas in a highly elongated harmonic trap

Xia-Ji Liu,[1] Hui Hu,[1,2] and Peter D. Drummond[1]
[1]*ARC Centre of Excellence for Quantum-Atom Optics, Department of Physics, University of Queensland, Brisbane, Queensland 4072, Australia*
[2]*Department of Physics, Renmin University of China, Beijing 100872, China*
(Received 27 November 2007; revised manuscript received 10 April 2008; published 1 August 2008)

We investigate the finite-temperature properties of an ultracold atomic Fermi gas with spin population imbalance in a highly elongated harmonic trap. Previous studies at zero temperature showed that the gas stays in an exotic spatially inhomogeneous Fulde-Ferrell-Larkin-Ovchinnikov (FFLO) superfluid state at the trap center; while moving to the edge, the system changes into either a nonpolarized Bardeen-Cooper-Schrieffer superfluid ($P<P_c$) or a fully polarized normal gas ($P>P_c$), depending on the smallness of the spin polarization P, relative to a critical value P_c. In this work, we show how these two phase-separation phases evolve with increasing temperature, and thereby construct a finite-temperature phase diagram. For typical interactions, we find that the exotic FFLO phase survives below one-tenth of Fermi degeneracy temperature, which seems to be accessible in the current experiment. The density profile, equation of state, and specific heat of the polarized system have been calculated and discussed in detail. Our results are useful for the ongoing experiment at Rice University on the search for FFLO states in quasi-one-dimensional polarized Fermi gases.

DOI: 10.1103/PhysRevA.78.023601 PACS number(s): 03.75.Ss, 05.30.Fk, 71.10.Pm, 74.20.Fg

I. INTRODUCTION

Impressive experimental progress has occurred recently in the field of ultracold Fermi gases. In particular, experimental realizations of the crossover from a Bardeen-Cooper-Schrieffer (BCS) superfluid to Bose-Einstein condensate (BEC) using a well-controlled Feshbach resonance [1–7] have opened an intriguing opportunity to study long-standing many-body problems in condensed matter physics, such as high-temperature superconductivity. Most recently, two experimental groups at Rice University and MIT have successfully manipulated a two-component atomic Fermi gas of lithium atoms with unequal spin populations [8–13]. This type of matter is of great interest, and stimulates intense efforts on studying an unsolved problem in condensed matter and particle physics: what is the ground state of a spin-polarized Fermi gas with attractive interactions?

Without spin polarization, the answer is known, given fifty years ago by Bardeen, Cooper, and Schrieffer. Due to attractions, atoms of different spin species at the same Fermi surface with opposite momentum form Cooper pairs characteristic of bosons, and thus undergo a BEC-like superfluid phase transition at a sufficiently low temperature. This BCS mean-field picture is very robust and is valid not only quantitatively at weak coupling, but also qualitatively in the strongly interacting limit [7], where the fluctuations of Cooper pairs become important. The key ingredient of the BCS pairing is the fully overlapped Fermi surfaces, which create a maximum for the phase space. In the presence of spin polarization, however, the two Fermi surfaces are no longer aligned. The standard Cooper pairing scheme is thus not applicable. For a small number of unpaired atoms or a small spin polarization, some nonstandard pairing scenarios have to be developed. For a large spin polarization above threshold, these unpaired atoms will eventually destroy the coherence of pairs and hence the superfluidity.

The determination of nonstandard pairing scenarios and the related exotic superfluidity lies at the heart of polarized Fermi gases. A number of pairing proposals have already been suggested in the literature, including breached pairing [14] or Sarma superfluidity [15,16], phase separation [17], deformed Fermi surface [18], and spatially modulated Fulde-Ferrell-Larkin-Ovchinnikov (FFLO) states [19,20]. At the moment, a theoretical consensus on the true ground state of a three-dimensional spin-polarized Fermi system is yet to be reached [21–27]. Experimental observations near a Feshbach resonance are not so helpful as one would expect, due to the presence of the harmonic trap. To take it into account, the local density approximation has been widely used [28–34], as well as the mean-field Bogoliubov–de Gennes equation [35–37].

Among various pairing schemes, the study of FFLO phases has the longest history—more than four decades [19,20]. In this scenario, the two mismatched Fermi surfaces have been shifted by an amount in momentum space [19], in order to have a small overlap of the surface. As a result, Cooper pairs with a finite center-of-mass momentum may form, and thereby support, a spatially inhomogeneous superfluidity [20]. However, due to the much reduced phase space for pairing, the window for the appearance of FFLO states turns out to be small in three dimensions [21,22]. This makes the experimental search for the FFLO states extremely challenging. Up to now only indirect evidence has been observed in the heavy fermion superconductor $CeCoIn_5$ [38]. No FFLO signal has been found in ultracold polarized atomic Fermi gases.

Luckily, the FFLO states are theoretically found to be favorable in low dimensions, which can be realized experimentally using an optical lattice [39]. In one dimension (1D), where the whole Fermi surface shrinks to two Fermi points, the reduction of pairing phase space is less significant. Consequently, at zero temperature the FFLO phase becomes

much more robust [40–42], compared to its 3D counterpart [22]. This expectation was indeed found in recent works [43–48]. Further, the presence of a harmonic trap will not change the essential picture, as first shown by Orso [45] and the present authors [46,47]. Nonetheless, the trap leads to phase separation [45,46]: While the system remains always in the FFLO phase at the trap center, at the trap edge, it can be either a fully nonpolarized BCS state or a fully polarized normal state, for small or large spin polarization, respectively. Most recently, the spatial distribution of pair correlation functions and the momentum distribution of a spin-polarized 1D Fermi gas in lattices have been investigated by using numerically accurate density-matrix renormalization-group methods [49–51] and quantum Monte Carlo simulations [52].

Inspired by theoretical suggestions, an experiment with polarized Fermi gases in a highly elongated harmonic trap is now underway at Rice University [53]. However, the experiment will necessarily be carried out at finite temperature. It is then desirable to understand how the two phase separation phases found at zero temperature evolve as temperature increases and, in particular, what is the temperature window for the presence of FFLO states, compared to the lowest experimentally attainable temperature.

In a previous study [47], we presented a systematic study of zero-temperature quantum phases in a one-dimensional spin-polarized Fermi gas. Three theoretical methods have been comparatively used: mean-field theory with either an order parameter in a single-plane-wave form or a self-consistently determined order parameter using the Bogoliubov–de Gennes equations [35–37,54–58], as well as the exact Bethe ansatz method [59]. We have found that a spatially inhomogeneous FFLO, which lies between the fully paired BCS state and the fully polarized normal state, dominates most of the phase diagram of a uniform gas. The phase transition from the BCS state to the FFLO phase is of second order. We have also investigated the effect of a harmonic trapping potential on the phase diagram, and find that in this case the trap generally leads to phase separation as mentioned above. We finally investigate the local fermionic density of states of the FFLO phase. A two-energy-gap structure is shown up, which may be used as an experimental probe of the FFLO states.

In this work, we address the urgent finite-temperature problem by extending our previous zero-temperature analysis. In particular, we focus on the use of weak-coupling Bogoliubov–de Gennes (BdG) theory [35,54,56]. Based on this mean-field approach we are able to obtain the density profiles of the system at finite temperatures, as well as its thermodynamic properties, including the entropy, energy, and specific heat.

Our main result, a finite temperature phase diagram, is shown in Fig. 1 for a typical interaction strength. At a finite but low temperature, in addition to the two phase separation states mentioned earlier, two new phases—a pure BCS state and a partially polarized normal state—enter the phase diagram, respectively, at lower and higher spin polarizations. The space for the phase separation states shrinks with increasing temperature and vanishes completely at one-fifth of the Fermi temperature T_F. Therefore, even at a temperature as high as $0.1T_F$, it is still possible to observe the long-sought FFLO state at the center of the harmonic trap. This suggests that the FFLO state in 1D polarized Fermi gases is indeed attainable with current experimental techniques [7].

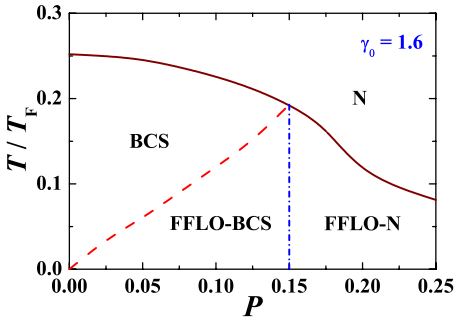

FIG. 1. (Color online) Finite temperature phase diagram of a 1D trapped spin-polarized Fermi gas at a given coupling constant $\gamma_0 = 1.6$ as a function of the spin polarization $P=(N_\uparrow - N_\downarrow)/(N_\uparrow + N_\downarrow)$, where $N_\uparrow$ and $N_\downarrow$ are the number of spin-up and spin-down atoms, respectively. T_F is the Fermi temperature of an ideal, noninteracting Fermi gas in a harmonic trap. The solid line gives the boundary of the second-order phase transition from a superfluid to a normal state. The dashed and dot-dashed lines distinguish the different superfluid phases: a pure BCS phase, a phase separation with a FFLO at center, and a BCS outside (FFLO-BCS), and a phase separation with FFLO and normal components (FFLO-N). Due to the presence of harmonic traps, these boundaries may be better understood as crossover, rather than phase transition lines.

In the following section, we briefly review the mean-field BdG theory of the 1D spin-polarized Fermi gas. The applicability of the mean-field theory in the weakly coupling or intermediate coupling regimes will be commented. In Sec. III, we will discuss in detail how the density profiles and the order parameters evolve with increasing temperatures. Together with the analysis of the entropy, energy, and specific heat, we obtain a phase diagram at finite temperatures. Finally, Sec. IV is devoted to the conclusions and remarks.

II. SELF-CONSISTENT BOGOLIUBOV–DE GENNES THEORY

Fermi gases of ^{6}Li atoms near a broad Feshbach resonance can be well described using a single channel model, as confirmed both experimentally [60] and theoretically [61,62]. To obtain the phase diagram in Fig. 1, we use the self-consistent BdG theory [54–56], by assuming a pairing order parameter $\Delta(x)$ that breaks the U(1) symmetry of the number conservation of total neutral atoms. This weak-coupling theory has been previously applied to discuss the zero-temperature properties of 1D polarized Fermi gases by the present authors. We refer to Ref. [47] for the detailed description of the model and the BdG formalism. We outline below some essential ingredients of the theory.

The BdG equations describing the quasiparticle wave functions $u_\eta(x)$ and $v_\eta(r)$, with excitation energies E_η are [54]

$$\begin{bmatrix} \mathcal{H}_{\uparrow}^{s} - \mu_{\uparrow} & -\Delta(x) \\ -\Delta^{*}(x) & -\mathcal{H}_{\downarrow}^{s} + \mu_{\downarrow} \end{bmatrix} \begin{bmatrix} u_{\eta}(x) \\ v_{\eta}(x) \end{bmatrix} = E_{\eta} \begin{bmatrix} u_{\eta}(x) \\ v_{\eta}(x) \end{bmatrix}, \quad (1)$$

where the single particle Hamiltonian $\mathcal{H}_{\sigma}^{s} = -\hbar^2\nabla^2/2m + g_{1D}n_{\bar{\sigma}}(x) + V_{\text{ext}}(x)$ and $V_{\text{ext}}(x) = m\omega^2 x^2/2$ is the harmonic trap potential. The interaction is a short-range potential $g_{1D}\delta(x)$, resulting in a diagonal Hartree term $g_{1D}n_{\bar{\sigma}}(x)$ and an off-diagonal order parameter potential in the mean-field decoupling. To account for the unequal spin population N_{σ} for the pseudospins $\sigma = \uparrow, \downarrow$, the chemical potentials are shifted as $\mu_{\uparrow,\downarrow} = \mu \pm \delta\mu$. This leads to different quasiparticle wave functions for the two spin components. However, there is a symmetry of the BdG equations under the replacement $u_{\eta\downarrow}^{*}(x) \to v_{\eta\uparrow}(x)$, $v_{\eta\downarrow}^{*}(x) \to -u_{\eta\uparrow}(x)$, $E_{\eta\downarrow} \to -E_{\eta\uparrow}$. Thus, in Eq. (1) we have kept only the spin-up part, and obtained the solutions with both positive and negative excitation energies.

The order parameter and the particle density of each component that appears in the BdG equations can be written as

$$\Delta(x) = -g_{1D}\sum_{\eta} u_{\eta}(x)v_{\eta}^{*}(x)f(E_{\eta}), \quad (2)$$

$$n_{\uparrow}(x) = \sum_{\eta} u_{\eta}^{*}(x)u_{\eta}(x)f(E_{\eta}), \quad (3)$$

$$n_{\downarrow}(x) = \sum_{\eta} v_{\eta}^{*}(x)v_{\eta}(x)f(-E_{\eta}), \quad (4)$$

where $f(E_{\eta}) = 1/(\exp[E_{\eta}/k_BT] + 1)$ is the Fermi distribution function. The particle density of each component is subjected to the constraint $\int dx n_{\sigma}(x) = N_{\sigma}$, which eventually determines the chemical potentials. Equation (1), together with the definitions of the order parameter and particle densities (2)–(4), form a closed set of equations, which has to be solved self-consistently. We have done so via a hybrid procedure, in which the high-lying excitation levels above an energy cutoff E_c has been solved approximately using a local density approximation. This procedure is very efficient. We refer to Refs. [47,55] for further details. Note that the final numerical results are independent of the cutoff energy E_c, provided that it is large enough.

Once the BdG equations are solved, it is straightforward to calculate the total entropy and total energy of the system. The expression for the entropy is given by

$$S = -k_B\sum_{E_{\eta}} [f(E_{\eta})\ln f(E_{\eta}) + f(-E_{\eta})\ln f(-E_{\eta})], \quad (5)$$

where the summation can be restricted to energy levels with energy $|E_{\eta}| \leqslant E_c$. Other high-lying branches have an exponentially small contribution because of the large value of $E_c (\gg k_BT)$. This has been neglected. In contrast, the total energy includes two parts $E = E_{\text{disc}} + E_{\text{cont}}$. The discrete contribution E_{disc} takes the form

$$E_{\text{disc}} = \left[\mu_{\uparrow}N_{\uparrow} + \mu_{\downarrow}N_{\downarrow} - g_{1D}\int dx|\Delta(x)|^2\right] + \sum_{|E_{\eta}| \leqslant E_c} E_{\eta}\left[f(E_{\eta}) - \int dx|v_{\eta}(x)|^2\right], \quad (6)$$

while the high-lying levels contribute

$$E_{\text{cont}} = \int dx[e_1(x) + e_2(x)], \quad (7)$$

where $e_1(x)$ and $e_2(x)$ are given by

$$e_1(x) = -\frac{(2m)^{1/2}}{4\pi\hbar}\int_{E_c}^{\infty} \epsilon d\epsilon \left[\frac{\epsilon + \delta\mu}{\sqrt{(\epsilon + \delta\mu)^2 - \Delta^2(x)}} - 1\right] \times \frac{1}{[\mu - V_{\text{ext}}(x) + \sqrt{(\epsilon + \delta\mu)^2 - \Delta^2(x)}]^{1/2}} \quad (8)$$

and

$$e_2(x) = -\frac{(2m)^{1/2}}{4\pi\hbar}\int_{E_c}^{\infty} \epsilon d\epsilon \left[\frac{\epsilon - \delta\mu}{\sqrt{(\epsilon - \delta\mu)^2 - \Delta^2(x)}} - 1\right] \times \frac{1}{[\mu - V_{\text{ext}}(x) + \sqrt{(\epsilon - \delta\mu)^2 - \Delta^2(x)}]^{1/2}}, \quad (9)$$

respectively. An important self-consistency check of the calculations of the entropy and of the energy is given by the thermodynamic relation

$$E(T) = E_0 + \int_0^T dT' T'\left(\frac{\partial S}{\partial T'}\right), \quad (10)$$

where E_0 is the ground-state energy at zero temperature.

Before closing the section, we discuss briefly the applicablity of mean-field Bogoliubov–de Gennes theory in one dimension. It is well known that with decreasing dimensionality, the pair fluctuation becomes increasingly important. Specifically to 1D, the true long-range order is completely destroyed by fluctuations. Thus, strictly speaking, there is no *a priori* justification for the use of mean-field BdG theory for a uniform spin-polarized Fermi gases. Nevertheless, we found in the previous study that at zero temperature and at a coupling constant $\gamma \sim 1$, the mean-field BdG calculation provides reasonable description for the energy and chemical potential of a uniform spin-polarized Fermi gas, as compared to the exact Bethe ansatz solutions (see, for example, Figs. 12 and 13 in Ref. [47]).

On the other hand, the presence of a harmonic trap effectively increases the dimensionality of the system. For instance, the density of state of the trapped 1D system is a constant, exhibiting the same behavior as a uniform Fermi gas in two dimensions. Thus, in a harmonic trap, we anticipate that the pair fluctuations should be much suppressed, and thus the use of the mean-field BdG theory may be justified. We have checked in the previous work the validity of BdG theory for a trapped spin-polarized Fermi gas and found that indeed, at $\gamma \sim 1$ the density profile of a trapped gas obtained from the zero-temperature BdG calculations agrees

well with that from the asymptotically exact Gaudin solutions (see, for example, Fig. 18 in Ref. [47]).

III. RESULTS AND DISCUSSIONS

For concreteness, we consider a trapped polarized gas with a number of total atoms $N=N_\uparrow+N_\downarrow=100$. In traps, it is convenient to take trap units with $m=\hbar=\omega=k_B=1$ so that the length and energy will be measured in units of the harmonic oscillator length $a_{Ho}=\sqrt{\hbar/m\omega}$ and of the level spacing $\hbar\omega$, respectively. The characteristic energy scale may be given by the Fermi energy of an unpolarized ideal gas at zero temperature $E_F=N\hbar\omega/2$, which also provides a characteristic temperature scale $T_F=E_F/k_B$. On the other hand, the length scale is set by a Thomas-Fermi radius $x_{\mathrm{TF}}=N^{1/2}a_{Ho}$. To characterize the interaction, we use a dimensionless coupling constant at the trap center [47] $\gamma_0=a_{Ho}/(\pi N^{1/2}a_{1\mathrm{D}})$, where $a_{1\mathrm{D}}=-mg_{1\mathrm{D}}/(n\hbar^2)$ is the 1D scattering length and γ_0 is roughly the ratio of the interaction energy density at the trap center to the kinetic energy density. Thus, $\gamma_0\ll 1$ corresponds to the weakly interacting limit, while the strong-coupling regime is realized when $\gamma_0\gg 1$. Throughout the paper, we use a coupling constant $\gamma_0=1.6$, comparable to the estimates for a real experimental setup [47].

A. Density profiles and order parameter

Figures 2 and 3 give BdG results for the density profiles of each component, as well as the density difference $\delta n(x)=n_\uparrow(x)-n_\downarrow(x)$ and the order parameter $\Delta(x)$, at different temperatures as indicated and at two spin polarizations $P=(N_\uparrow-N_\downarrow)/N=0.075$ (Fig. 2) and 0.175 (Fig. 3). In the work by Orso [45] and our previous studies [46,47], it was shown that at zero temperature there are two phase separation states: For a small spin polarization the system stays in the spatially inhomogeneous FFLO superfluid state at the trap center and in a BCS superfluid state at the edge (referred to as FFLO-BCS later). For a large spin polarization, the gas still remains in the FFLO state at the trap center, but becomes a fully polarized normal state towards the edge of the trap (referred to as FFLO-N later). We refer to the Secs. VI and VII A of Ref. [47] for further details. The two spin polarizations in Figs. 2 and 3 are selected in such a way that initially (at low temperature) the cloud is in different phase separation ground state. We then trace how these two phase separation states develop as the temperature increases.

For a small spin polarization below a critical value P_c, the FFLO-BCS phase separation state at low temperature is clearly characterized by the spatial profile of the order parameter [Fig. 2(a)]. It shows oscillations at the trap center, characteristic of FFLO states, and two shoulders at the trap edge, characteristic of a 1D BCS state. Naively, the FFLO state is much more easily disturbed by thermal fluctuations than the BCS state, due to a reduced pairing phase space. Therefore, as shown in Figs. 2(b) and 2(c), with increasing temperature the FFLO superfluid is suppressed faster than the BCS shoulders at the edge. This leads to a pure BCS state above a certain temperature about $0.10T_F$. Further increase of the temperature will destroy the superfluid state eventually at around $0.20T_F$.

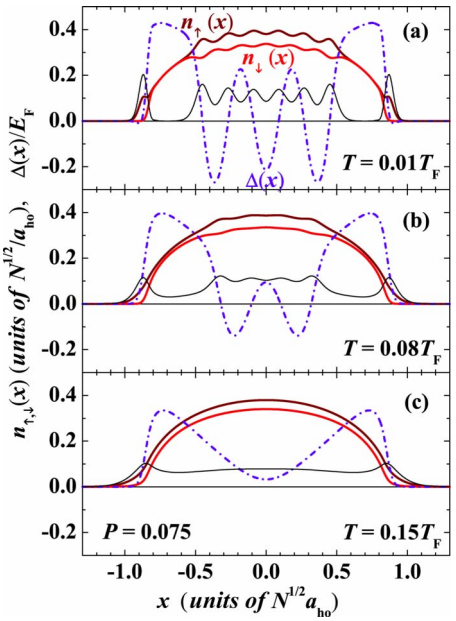

FIG. 2. (Color online) Spin-up and spin-down density profiles (thick solid lines), the density difference (thin solid lines), and the order parameter (dot-dashed lines) of a trapped 1D Fermi gas for a spin polarization $P=0.075$, at several temperatures $T=0.01T_F$ (upper panel), $T=0.08T_F$ (middle panel), and $T=0.15T_F$ (bottom panel). For a better illustration, the scale of the density difference has been doubled. At zero temperature, the system stays in a phase separation phase with a FFLO state at center and an outside BCS shell. The FFLO phase at the trap center, signaled by the oscillations in the order parameter, suppresses with increasing temperature, and leaves out a pure BCS state throughout the trap at about $0.10T_F$. At a higher temperature around $0.20T_F$, the system becomes fully normal through a second-order superfluid phase transition.

Experimentally, the change from FFLO-BCS phase separation state to the pure BCS state and finally to the normal state may be monitored by measuring the density difference. At low temperature in the FFLO-BCS separation phase, the local spin polarization or density difference is fully carried by the FFLO state and thus is restricted to the trap center [Fig. 2(a)]. Here, we have neglected the single peak of density difference exactly at the trap edge that is caused by breakdown of the mean-field approach, see Ref. [47] for detailed discussions. At a higher temperature, the BCS state starts to contribute to the spin polarization, due to the thermal excitations. As a result, the density difference leaks out gradually to the trap edge [Fig. 2(b)]. When the FFLO state fully disappears, the difference in density becomes very flat throughout the trap [Fig. 2(c)].

The temperature evolution for a FFLO-N phase separation state with large spin polarizations is simpler, as shown in Fig. 3. In this case, the FFLO state at the trap center is destroyed gradually by increasing temperature, and one ends up with a fully normal cloud around $T\simeq 0.15T_F$. The shape of density difference profiles is nearly independent of temperature. Thus, the distinct temperature dependence of the density difference in the FFLO-BCS and FFLO-N states provides a useful way to distinguish these two phase separation phases.

At the end of this subsection, we emphasize that in Figs. 2(a) and 2(b) it is the oscillation of the order parameter that

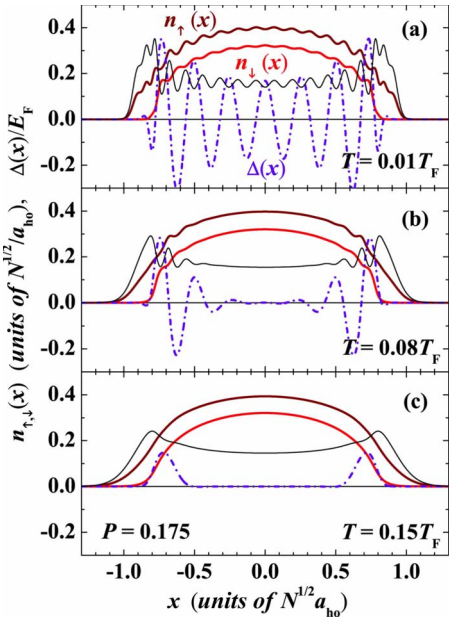

FIG. 3. (Color online) Same plots as in Fig. 2, but for a larger spin polarization $P=0.175$. With this value of spin polarizations, at zero temperature the atoms at the trap edge stay in a normal state. With increasing temperature, the FFLO phase at the trap center vanishes gradually, which eventually leads to a normal phase throughout the trap at $T \simeq 0.15T_F$.

is the unambiguous signature of the FFLO state. There is also a related oscillation in the density profiles with doubling periodicity. However, these density oscillations are presumably due to finite size effect. We have checked this point by varying the number of total atoms. In Figs. 4 and 5, we show the density difference and the order parameter at a spin polarization $P=0.175$ and at a low temperature $T=0.01T_F$ for particle numbers in the range 50–200. With increasing number of total atoms, the amplitude of the density oscillation at the trap center becomes smaller. In contrast, the amplitude of the order parameter $\Delta(x=0)$ stays nearly constant. Note that in Fig. 5 we find a Larkin-Ovchinnikov (LO) state in the center region, i.e., the order parameter behaves as $\Delta(x) = \Delta(x=0)\cos(q_{\mathrm{LO}}x)$ with a center-of-mass momentum q_{LO} proportional to the Fermi wave-vector difference, $q_{\mathrm{LO}} \simeq k_{F\uparrow} - k_{F\downarrow} \simeq (N^{1/2}P)a_{Ho}^{-1}$. Thus, in units of $(N^{1/2}a_{Ho})$ the periodicity of the density oscillation [Fig. 4(c)] and of the order parameter are inversely proportional to the number of total atoms.

B. Equation of state

Figures 6 and 7 show the equation of state as a function of temperature. The total entropy and total energy increase monotonically with increasing temperature and spin polarization. In particular, at a finite spin polarization, the entropy increases linearly with temperature, as compared to the exponential temperature dependence for a BCS superfluid (i.e., $P=0$). This linear dependence arises from having gapless single-particle excitations located at the node of FFLO states at the trap center, and in case of the FFLO-N phase, from the normal cloud at the edge of the trap. As the temperature

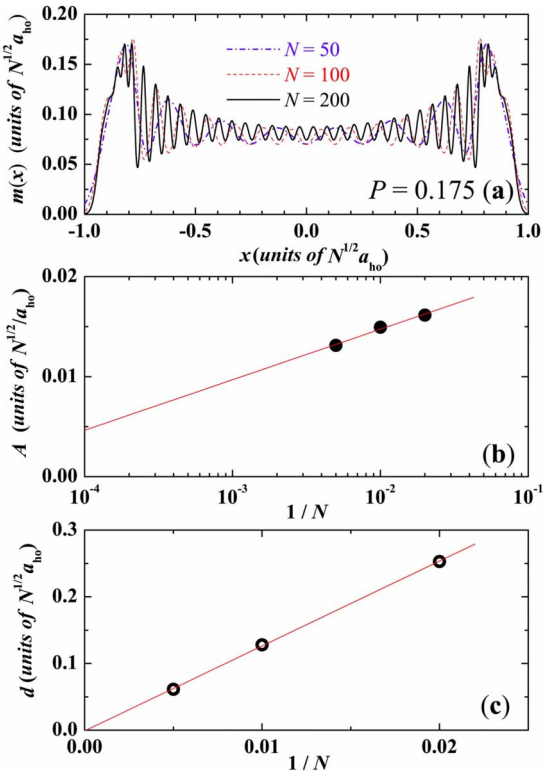

FIG. 4. (Color online) (a) Density difference of a spin-polarized Fermi gas at $P=0.175$ and $T=0.01T_F$ for different numbers of total atoms as indicated. (b) The number dependence of the amplitude of the density oscillations A at the trap center. The amplitude A decreases slowly with increasing the number of atoms. (c) The number dependence of the periodicity of the density oscillations d at the trap center.

increases, nontrivial kinks are visible in both chemical potentials and entropy, reflecting the smooth transitions between different states as mentioned earlier.

C. Specific heat and finite-temperature phase diagram

The analysis of the profiles of the density distributions and of the order parameter has already given some qualitative features for the phase diagram at finite temperatures. To quantify it, we calculate the specific heat, using the definition

$$C_V = \frac{\partial E}{\partial T} = T\frac{\partial S}{\partial T}. \tag{11}$$

Figure 8 displays the temperature dependence of the specific heat at three spin polarizations. Different transitions are well characterized by the apparent kinks in the specific heat. For a small polarization, two kinks are clearly visible, corresponding to the transition from a FFLO-BCS phase separation state to a pure BCS state, and in turn to a normal state. In contrast, for large polarization, typically only one kink is identifiable, which should be attributed to the transition from a FFLO-N phase separation state to a completely normal state.

Gathering the position (temperature) of the kinks for different spin polarizations, we obtain the solid and dashed lines in the phase diagram, as shown in Fig. 1. The former

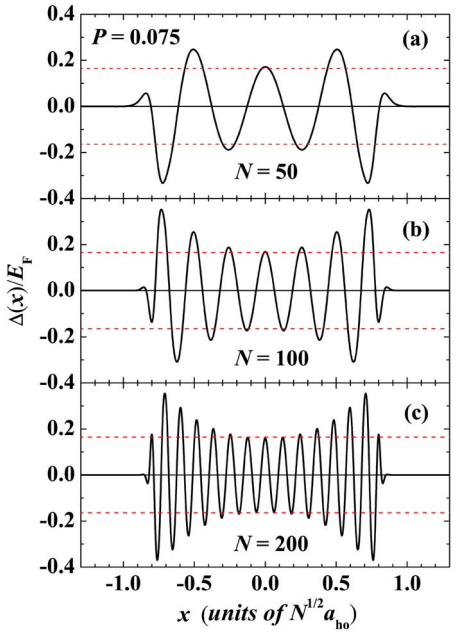

FIG. 5. (Color online) Order parameters of a spin-polarized Fermi gas at $P=0.175$ and $T=0.01T_F$ for different numbers of total atoms: (a) $N=50$, (b) $N=100$, and (c) $N=200$. The two dashed lines indicate the value of the order parameter at the trap center.

line corresponds to the second-order phase transition from either a BCS or FFLO-N to the normal state; while the later distinguishes a high-T pure BCS state from a low-T FFLO-BCS phase separation state. The determination of the boundary between FFLO-BCS and FFLO-N phase separation phases, for example, the critical spin polarization $P_c(T)$, is more difficult from numerics. As discussed in our previous works [46,47], the critical spin polarization is calculated from a critical chemical potential difference, i.e., half of the binding energy of the 1D molecule pairs. From Fig. 6(b), for a large spin polarization the chemical potential difference is temperature insensitive. On quite general grounds, we thus

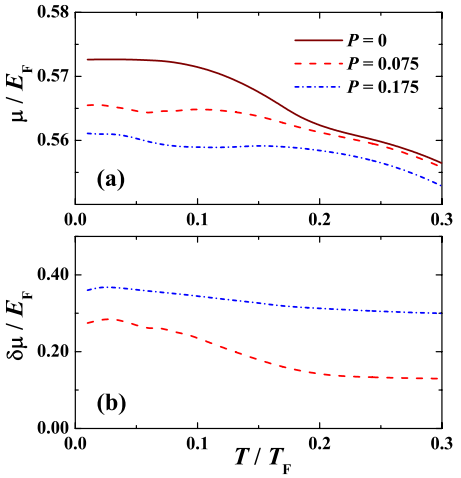

FIG. 6. (Color online) Temperature dependence of the chemical potential [panel (a)] and of the chemical potential difference [panel (b)] at three spin polarizations: $P=0$ (solid lines), 0.075 (dashed lines), and 0.175 (dash-dotted lines).

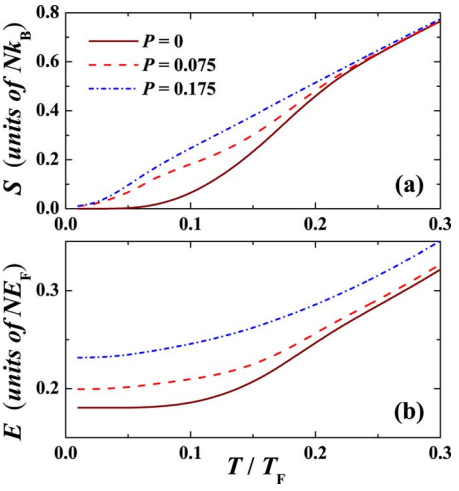

FIG. 7. (Color online) Temperature dependence of the total entropy per particle [panel (a)] and of the total energy per particle [panel (b)] at three spin polarizations: $P=0$ (solid lines), 0.075 (dashed lines), and 0.175 (dash-dotted lines).

assume that the critical spin polarization $P_c(T)$ is nearly temperature independent. This gives the dash-dotted line in the phase diagram (Fig. 1).

It is evident from Fig. 1 that there is a wide temperature window for the presence of FFLO states at the trap center. The typical temperature for observing the FFLO state would be one-tenth of the Fermi temperature, corresponding to an entropy $S\sim 0.2Nk_B$. Such a temperature or entropy is within the reach of present-day techniques [7].

IV. CONCLUDING REMARKS

In conclusion, based on a mean-field Bogoliubov–de Gennes theory, we calculate the thermodynamic properties of a polarized atomic Fermi gas in a highly elongated harmonic trap. The profiles of the density distributions and of order parameter, the equation of state, as well as the specific heat have been analyzed in detail. We have then established a finite temperature phase diagram. Our results are useful for

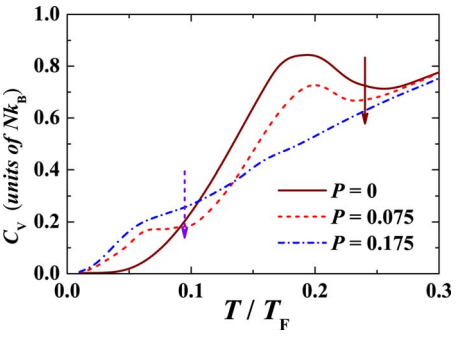

FIG. 8. (Color online) Temperature dependence of the specific heat at three spin polarizations: $P=0$ (solid line), 0.075 (dashed line), and 0.175 (dash-dotted line). For $P=0.075$, the dashed arrow indicates the transition from a FFLO-BCS phase separation phase to a pure BCS state, while the solid arrow marks the second-order phase transition from a BCS superfluid to a normal gas.

experiments at Rice University [53], in which a search for the exotic FFLO states in 1D polarized Fermi gases is undertaken. Our estimated temperature and entropy for the realization of FFLO states are about $0.1T_F$ and $0.2Nk_B$, respectively. These values are experimentally attainable [7].

While our weak-coupling Bogoliubov–de Gennes study provides a semiquantitative finite-temperature phase diagram of the 1D polarized Fermi gas, an improved description could be obtained by solving the exact thermodynamic Bethe ansatz solutions of the 1D gas [59], with the trap effect treated using a local density approximation [45,46]. We plan on doing this in future work.

ACKNOWLEDGMENTS

This research was supported by the Australian Research Council Center of Excellence, the National Natural Science Foundation of China Grant No. NSFC-10774190, and the National Fundamental Research Program of China Grant Nos. 2006CB921404 and 2006CB921306.

[1] C. A. Regal, M. Greiner, and D. S. Jin, Phys. Rev. Lett. **92**, 040403 (2004).
[2] M. W. Zwierlein, C. A. Stan, C. H. Schunck, S. M. F. Raupach, A. J. Kerman, and W. Ketterle, Phys. Rev. Lett. **92**, 120403 (2004).
[3] J. Kinast, S. L. Hemmer, M. E. Gehm, A. Turlapov, and J. E. Thomas, Phys. Rev. Lett. **92**, 150402 (2004).
[4] C. Chin, M. Bartenstein, A. Altmeyer, S. Riedl, S. Jochim, J. Hecker Denschlag, and R. Grimm, Science **305**, 1128 (2004).
[5] T. Bourdel, L. Khaykovich, J. Cubizolles, J. Zhang, F. Chevy, M. Teichmann, L. Tarruell, S. J. J. M. F. Kokkelmans, and C. Salomon, Phys. Rev. Lett. **93**, 050401 (2004).
[6] G. B. Partridge, K. E. Strecker, R. I. Kamar, M. W. Jack, and R. G. Hulet, Phys. Rev. Lett. **95**, 020404 (2005).
[7] H. Hu, P. D. Drummond, and X.-J. Liu, Nat. Phys. **3**, 469 (2007), and references therein.
[8] M. W. Zwierlein, A. Schirotzek, C. H. Schunck, and W. Ketterle, Science **311**, 492 (2006).
[9] G. B. Partridge, Wenhui Li, R. I. Kamar, Y. A. Liao, and R. G. Hulet, Science **311**, 503 (2006).
[10] G. B. Partridge, Wenhui Li, Y. A. Liao, R. G. Hulet, M. Haque, and H. T. C. Stoof, Phys. Rev. Lett. **97**, 190407 (2006).
[11] M. W. Zwierlein, C. H. Schunck, A. Schirotzek, and W. Ketterle, Nature (London) **442**, 54 (2006).
[12] Y. Shin, M. W. Zwierlein, C. H. Schunck, A. Schirotzek, and W. Ketterle, Phys. Rev. Lett. **97**, 030401 (2006).
[13] C. H. Schunck, Y. Shin, A. Schirotzek, M. W. Zwierlein, and W. Ketterle, Science **316**, 867 (2007).
[14] W. V. Liu and F. Wilczek, Phys. Rev. Lett. **90**, 047002 (2003).
[15] G. Sarma, J. Phys. Chem. Solids **24**, 1029 (1963).
[16] C.-H. Pao, S.-T. Wu, and S.-K. Yip, Phys. Rev. B **73**, 132506 (2006).
[17] P. F. Bedaque, H. Caldas, and G. Rupak, Phys. Rev. Lett. **91**, 247002 (2003).
[18] H. Müther and A. Sedrakian, Phys. Rev. Lett. **88**, 252503 (2002).
[19] P. Fulde and R. A. Ferrell, Phys. Rev. **135**, A550 (1964).
[20] A. I. Larkin and Y. N. Ovchinnikov, Zh. Eksp. Teor. Fiz. **47**, 1136 (1964) [Sov. Phys. JETP **20**, 762 (1965)].
[21] D. E. Sheehy and L. Radzihovsky, Phys. Rev. Lett. **96**, 060401 (2006).
[22] H. Hu and X.-J. Liu, Phys. Rev. A **73**, 051603(R) (2006).
[23] D. T. Son and M. A. Stephanov, Phys. Rev. A **74**, 013614 (2006).
[24] L. He, M. Jin, and P. Zhuang, Phys. Rev. B **73**, 214527 (2006).
[25] M. Iskin and C. A. R. Sá de Melo, Phys. Rev. Lett. **97**, 100404 (2006).
[26] X.-J. Liu and H. Hu, Europhys. Lett. **75**, 364 (2006).
[27] M. M. Parish, F. M. Marchetti, A. Lamacraft, and B. D. Simons, Nat. Phys. **3**, 124 (2007).
[28] F. Chevy, Phys. Rev. Lett. **96**, 130401 (2006).
[29] W. Yi and L.-M. Duan, Phys. Rev. A **73**, 031604(R) (2006); **73**, 063607 (2006); **74**, 013610 (2006).
[30] T. N. De Silva and E. J. Mueller, Phys. Rev. Lett. **97**, 070402 (2006).
[31] C. Lobo, A. Recati, S. Giorgini, and S. Stringari, Phys. Rev. Lett. **97**, 200403 (2006).
[32] C.-C. Chien, Q. Chen, Y. He, and K. Levin, Phys. Rev. Lett. **97**, 090402 (2006).
[33] A. Bulgac and M. McNeil Forbes, Phys. Rev. A **75**, 031605(R) (2007).
[34] M. Haque and H. T. C. Stoof, Phys. Rev. Lett. **98**, 260406 (2007).
[35] J. Kinnunen, L. M. Jensen, and P. Törmä, Phys. Rev. Lett. **96**, 110403 (2006).
[36] K. Machida, T. Mizushima, and M. Ichioka, Phys. Rev. Lett. **97**, 120407 (2006).
[37] X.-J. Liu, H. Hu, and P. D. Drummond, Phys. Rev. A **75**, 023614 (2007).
[38] H. A. Radovan, N. A. Fortune, T. P. Murphy, S. T. Hannahs, E. C. Palm, S. W. Tozer, and D. Hall, Nature (London) **425**, 51 (2003); A. Bianchi, R. Movshovich, C. Capan, P. G. Pagliuso, and J. L. Sarrao, Phys. Rev. Lett. **91**, 187004 (2003); C. Martin, C. C. Agosta, S. W. Tozer, H. A. Radovan, E. C. Palm, T. P. Murphy, and J. L. Sarrao, Phys. Rev. B **71**, 020503(R) (2005).
[39] H. Moritz, T. Stöferle, K. Guenter, M. Köhl, and T. Esslinger, Phys. Rev. Lett. **94**, 210401 (2005).
[40] K. Machida and H. Nakanishi, Phys. Rev. B **30**, 122 (1984).
[41] A. I. Buzdin and S. V. Polonskii, Zh. Eksp. Teor. Fiz. **93**, 747 (1987) [Sov. Phys. JETP **66**, 422 (1987)].
[42] K. Yang, Phys. Rev. B **63**, 140511(R) (2001), and references therein.
[43] M. T. Batchelor, M. Bortz, X. W. Guan, and N. Oelkers, J. Phys.: Conf. Ser. **42**, 5 (2006).
[44] X.-W. Guan, M. T. Batchelor, C. Lee, and M. Bortz, Phys. Rev. B **76**, 085120 (2007).
[45] G. Orso, Phys. Rev. Lett. **98**, 070402 (2007).
[46] H. Hu, X.-J. Liu, and P. D. Drummond, Phys. Rev. Lett. **98**, 070403 (2007).

[47] X.-J. Liu, H. Hu, and P. D. Drummond, Phys. Rev. A **76**, 043605 (2007).
[48] M. M. Parish, S. K. Baur, E. J. Mueller, and D. A. Huse, Phys. Rev. Lett. **99**, 250403 (2007).
[49] M. Tezuka and M. Ueda, Phys. Rev. Lett. **100**, 110403 (2008).
[50] A. E. Feiguin and F. Heidrich-Meisner, Phys. Rev. B **76**, 220508(R) (2007).
[51] A. Luscher, R. M. Noack, and A. M. Lauchli, e-print arXiv: 0712.1808.
[52] G. G. Batrouni, M. H. Huntley, V. G. Rousseau, and R. T. Scalttar, Phys. Rev. Lett. **100**, 116405 (2008).
[53] R. G. Hulet (private communication).
[54] P. de Gennes, *Superconductivity of Metals and Alloys* (Addison-Wesley, New York, 1966).
[55] J. Reidl, A. Csordás, R. Graham, and P. Szépfalusy, Phys. Rev. A **59**, 3816 (1999).
[56] G. M. Bruun, Y. Castin, R. Dum, and K. Burnett, Eur. Phys. J. D **7**, 433 (1999); G. M. Bruun and H. Heiselberg, Phys. Rev. A **65**, 053407 (2002).
[57] N. Nygaard, G. M. Bruun, C. W. Clark, and D. L. Feder, Phys. Rev. Lett. **90**, 210402 (2003).
[58] M. Grasso and M. Urban, Phys. Rev. A **68**, 033610 (2003).
[59] M. Takahashi, *Thermodynamics of One-Dimensional Solvable Models* (Cambridge University Press, Cambridge, 1999).
[60] G. B. Partridge, K. E. Strecker, R. I. Kamar, M. W. Jack, and R. G. Hulet, Phys. Rev. Lett. **95**, 020404 (2005).
[61] R. B. Diener and Tin-Lun Ho, e-print arXiv:cond-mat/0405174.
[62] X.-J. Liu and H. Hu, Phys. Rev. A **72**, 063613 (2005).